

# Computational Analysis of Cyclophane-Based Bisthiourea-Catalyzed Henry Reactions

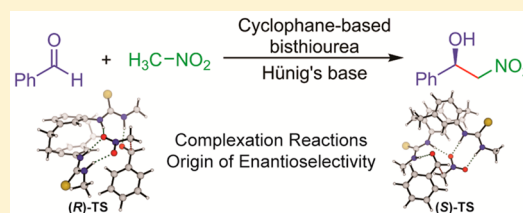
Martin Breugst<sup>\*,†,‡</sup> and K. N. Houk<sup>\*,‡</sup>

<sup>†</sup>Department für Chemie, Universität zu Köln, Greinstraße 4, 50939 Köln, Germany

<sup>‡</sup>Department of Chemistry and Biochemistry, University of California, Los Angeles, California 90095-1569, United States

**S** Supporting Information

**ABSTRACT:** The Henry reaction between benzaldehyde and nitromethane catalyzed by a cyclophane-based bisthiourea has been studied with density functional theory [M06-2X-D3/def2-TZVPP/IEFPCM//TPSS-D2/6-31G(d)/IEFPCM]. The results of our study reveal that the transformation involves the reaction of a thiourea–nitronate complex with the uncoordinated aldehyde. On the basis of our calculations, the formation of the major stereoisomer is kinetically preferred. Employing smaller model systems, we show that the observed stereoselectivity arises primarily from differences in hydrogen bonding in diastereomeric transition states.



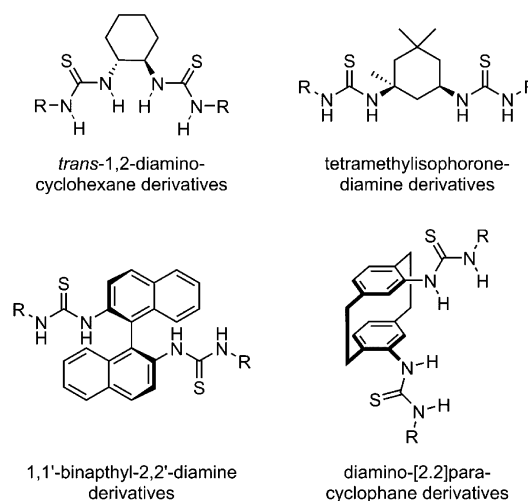
## INTRODUCTION

Building on initial reports by the groups of Kelly,<sup>1</sup> Etter,<sup>2</sup> Curran,<sup>3</sup> and others in the 1990s about the activation of electrophiles via hydrogen bonding, Jacobsen and co-workers realized the potential of (thio)urea catalysts for stereoselective reactions in the course of their work on asymmetric Strecker reactions.<sup>4</sup> A few years later, Schreiner and co-workers systematically investigated the reactivities of differently substituted thioureas as catalysts for Diels–Alder reactions.<sup>5</sup> Over the past decades, different research groups have successfully applied a large number of thiourea-derived catalysts for many different reactions, including Morita–Baylis–Hillman, Mannich, Henry, and Diels–Alder reactions.<sup>6</sup>

The simultaneous activation of both the nucleophile and the electrophile in enzyme catalysis<sup>7</sup> has inspired the development of a variety of bifunctional catalysts by combining a thiourea substructure with amines or a second thiourea subunit.<sup>4a,8</sup> Among the chiral bisthiourea catalysts, most have relied on *trans*-1,2-diaminocyclohexane,<sup>9</sup> tetramethylisophoronediamine,<sup>10</sup> or 1,1'-binaphthyl-2,2'-diamine backbones (Scheme 1).<sup>11</sup>

Recently, Kitagaki, Ueda, and Mukai examined the scope of the planar chiral [2.2]paracyclophane backbone for bisthiourea catalysts,<sup>12</sup> extending earlier studies by Paradies and co-workers.<sup>13</sup> They reported on the Henry reaction between differently substituted aldehydes (e.g., 1) and nitroalkanes (e.g., 2–H) catalyzed by cyclophane-based bisthiourea 3a (Scheme 2).<sup>12</sup> Following previous suggestions by Sohtome and Nagasawa on thiourea-catalyzed Morita–Baylis–Hillman reactions,<sup>14</sup> it was speculated that the high enantioselectivities observed in these reactions could result from dual activation (coordination of the nitronate by one thiourea subunit and the aldehyde by the second) and different steric crowding at the diastereomeric transition states.

## Scheme 1. Motifs for Bisthiourea Catalysts

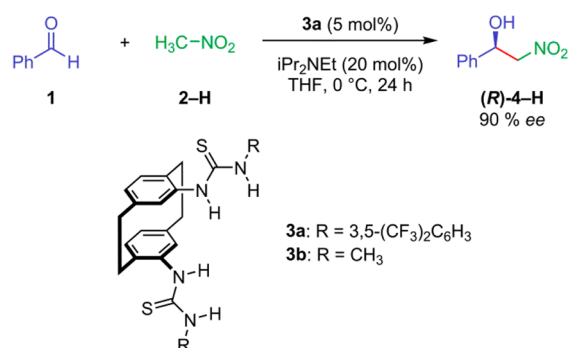


As the design of new organocatalysts relies on a detailed understanding of the underlying factors controlling the stereochemistry in these reactions, we undertook a computational analysis of the thiourea-catalyzed Henry reaction employing density functional theory (DFT). We now report on the results of our calculations and elucidate the origin of the observed enantioselectivity. In the following analysis, we will first discuss the uncatalyzed background reaction and then present a thorough analysis of all of the putative reactant complexes. Subsequently, we will describe our results for the thiourea-catalyzed reaction and rationalize the observed enantioselectivities on the basis of smaller model systems.

Received: June 2, 2014

Published: June 13, 2014

### Scheme 2. Cyclophane-Based Bisthiourea-Catalyzed Asymmetric Henry Reaction (from Reference 12)



## RESULTS AND DISCUSSION

**Uncatalyzed Henry Reaction.** In order to compare the thiourea-catalyzed reaction with the uncatalyzed Henry reaction, we first calculated the activation free energy for the nucleophilic attack of nitronate anion (**2**) on benzaldehyde (**1**) as well as the thermodynamics of the overall reaction (Figure 1).

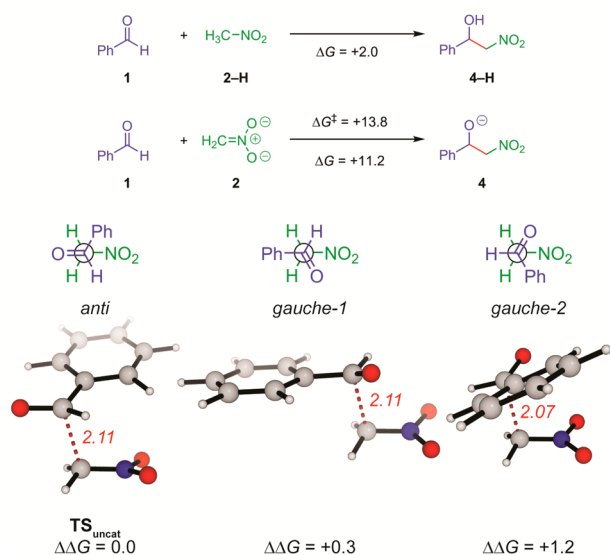


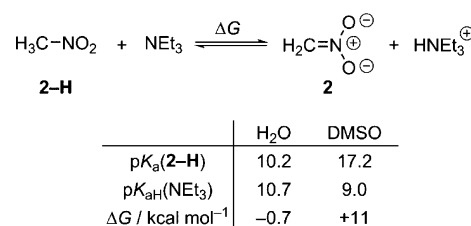
**Figure 1.** Transition states, reaction free energies, and activation free energies [in kcal mol<sup>-1</sup>; M06-2X-D3/def2-TZVPP/IEFPCM//TPSS-D2/6-31G(d)/IEFPCM] for the Henry reaction between benzaldehyde (**1**) and nitromethane (**2-H**) or the corresponding nitronate anion **2**.

In line with previous experimental<sup>15</sup> and computational<sup>16</sup> studies, the nucleophilic attack of the nitronate on the aldehyde was calculated to proceed through  $\text{TS}_{\text{uncat}}$  ( $\Delta G^\ddagger = 13.8$  kcal mol<sup>-1</sup>; Figure 1) featuring an *anti* orientation of the carbonyl and nitro groups. Corresponding transition states with *gauche* conformations were located slightly higher in energy (Figure 1). Both the attack of nitronate anion **2** on benzaldehyde to yield alcoholate **4** and the overall reaction to yield **4-H** are (slightly) endergonic, which is in agreement with the reversibility of Henry reactions.<sup>17</sup> The nitro compound **2-H** is more acidic than the alcohol **4-H**. The results of our calculations are in line with previous B3LYP calculations by Himo and co-workers, who determined a reaction free energy of +1.2 kcal mol<sup>-1</sup> (-0.7 kcal mol<sup>-1</sup> in the gas phase) for the overall reaction of Figure 1.<sup>18</sup> The small underestimation of the

thermodynamics in these reactions (i.e., the prediction of a slightly endergonic reaction instead of an exergonic reaction) has previously been observed for similar transformations such as aldol and Mannich reactions.<sup>19</sup>

Although no experimental data are available for the acidities of nitromethane (**2-H**) and the ammonium ion of Hünig's base in THF solution, we estimated the proton transfer of Scheme 3 to be almost thermoneutral in water and endergonic

### Scheme 3. Reaction Free Energies for the Deprotonation of Nitromethane and pK<sub>a</sub> Values (from Reference 20) in Water and DMSO



in DMSO on the basis of the acidities<sup>20</sup> of the triethylammonium ion (a model for the experimentally employed Hünig's base) and nitromethane in these solvents. While our calculations predict a high endergonicity for the proton transfer leading to the separated ions ( $\Delta G = 29.1$  kcal mol<sup>-1</sup>) due to charge separation, a reasonable free energy of proton transfer was determined for the formation of the ion pair of the ammonium ion and the nitronate **2** ( $\Delta G = 10.1$  kcal mol<sup>-1</sup>; cf.  $\Delta G$  in DMSO in Scheme 3). The accurate description of proton transfer reactions in THF solution is problematic because of the likelihood of specific solvent-solute interactions that are not taken into account in continuum models. We have assumed that all of the negatively charged complexes on the reaction path are similarly affected by ion pairing. Therefore, we base the following investigations mainly on the reactions of the nitronate anion and do not include ion pairing of the ammonium ion in our analysis.

**Complexation Reactions.** The bifunctional cyclophane-based organocatalyst is thought to bind both the aldehyde and the nitronate anion prior to the reaction.<sup>12,14</sup> Therefore, we first analyzed the thermodynamically most stable complexes formed between the model thiourea catalyst **3b** and benzaldehyde (**1**), neutral nitromethane (**2-H**), or nitronate anion **2**. The most stable complexes are depicted in Figure 2, and the corresponding complexation enthalpies and free energies are collected in Scheme 4.

While the *Z,Z* conformation of thioureas is often cited as an ideal arrangement for hydrogen bonding of nitro groups,<sup>6</sup> the *E,Z* conformer of **3b** is more stable by 6.0 kcal mol<sup>-1</sup> (2.0 kcal mol<sup>-1</sup> for **3a**). The corresponding *E,E* conformer of **3b** was located 5.8 kcal mol<sup>-1</sup> (0.4 kcal mol<sup>-1</sup> for **3a**) higher in energy. This result is in qualitative agreement with previous experimental and computational studies<sup>21</sup> on diaryl thiourea derivatives, which concluded that the *E,Z* conformer is slightly more stable at low temperatures.

Nevertheless, the *Z,Z* conformer is featured in the most stable bimolecular complex, **5-H**. This complex of thiourea **3b** and neutral nitromethane (**2-H**) is held together by three hydrogen bonds (1.95, 2.04, and 2.07 Å; Figure 2). The formation of this complex is exothermic but endergonic ( $\Delta H = -7.3$  kcal mol<sup>-1</sup>,  $\Delta G = +3.2$  kcal mol<sup>-1</sup>; not shown in Scheme

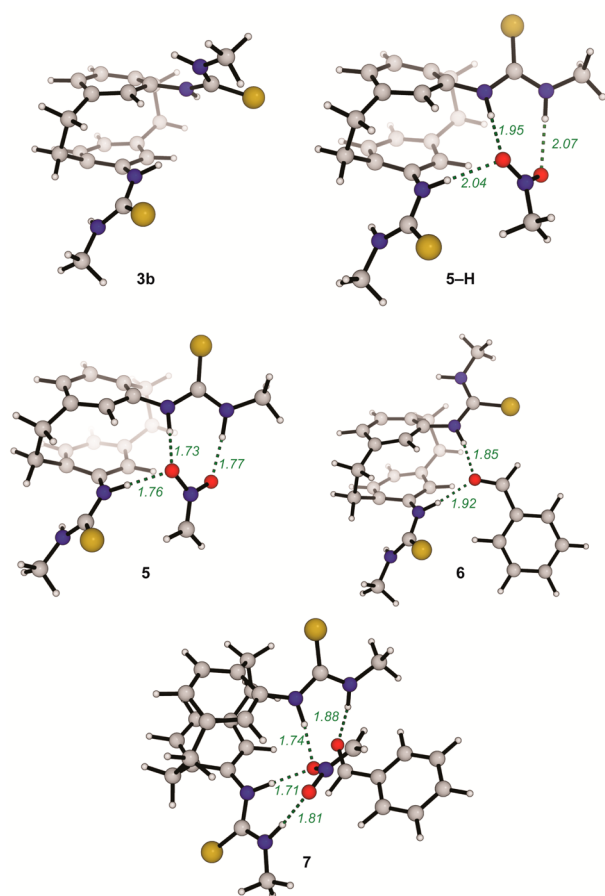


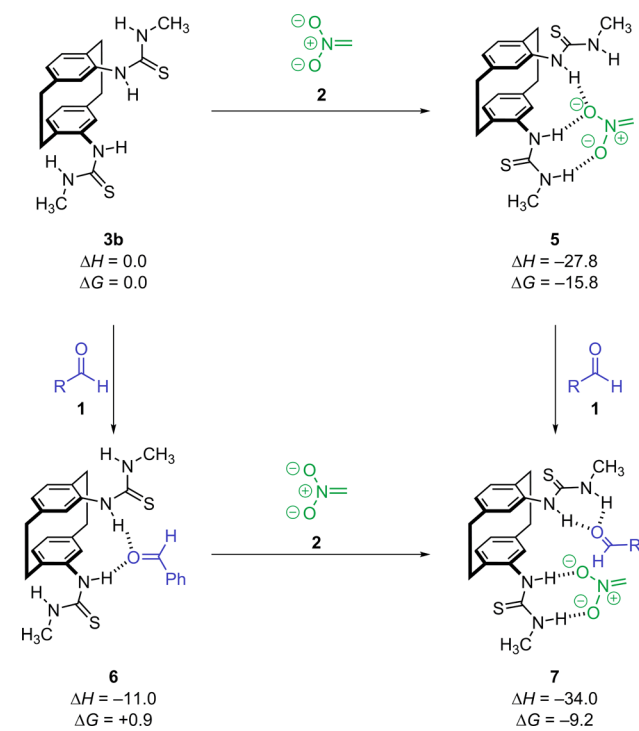
**Figure 2.** Lowest-energy structures [M06-2X-D3/def2-TZVPP/IEFPCM//TPSS-D2/6-31G(d)/IEFPCM] for the model thiourea catalyst **3b** and its adducts **5–7** with nitromethane (**2–H**), nitronate anion **2**, and aldehyde **1**.

4). Because of the endergonicity of this reaction (perhaps overestimated), **5–H** will not be present in large concentration.

Deprotonation of **5–H** gives nitronate–thiourea complex **5**, which has one *Z,Z* and one *E,Z* thiourea subunit and three hydrogen bonds. Because of the negative charge on the nitronate, the hydrogen bonds are relatively short in the bimolecular complex **5** (1.73, 1.76, and 1.77 Å; Figure 2) compared with the neutral analogue **5–H**. Slightly longer hydrogen bonds (ca. 1.9 Å) have previously been calculated for the cinchona thiourea-catalyzed Henry reaction in the gas phase,<sup>18</sup> reflecting the influence of solvation and dispersion effects in these reactions. The strong interaction is also reflected in the favorable enthalpy and free energy of formation of **5** ( $\Delta H = -27.8$  kcal mol<sup>-1</sup>,  $\Delta G = -15.8$  kcal mol<sup>-1</sup>; Scheme 4). An alternative orientation in which only one thiourea substructure is involved in hydrogen bonding was found to be 7.1 kcal mol<sup>-1</sup> higher in energy.

In complex **6**, the most stable complex formed from thiourea **3b** and benzaldehyde (**1**), the aldehyde is coordinated to both thiourea subunits in a bidentate fashion (1.85 and 1.92 Å; Figure 2). This complex is structurally similar to the crystal structure reported for the THF adduct of catalyst **3a**,<sup>12</sup> which supports our computational method. Comparable bond lengths have been calculated previously for similar reactions.<sup>18,22</sup> While the formation of the aldehyde–thiourea complex **6** is exothermic by 11.0 kcal mol<sup>-1</sup>, the bimolecularity of that reaction ( $-T\Delta S = 11.9$  kcal mol<sup>-1</sup>) renders the complexation

**Scheme 4.** Reaction Enthalpies and Free Energies [in kcal mol<sup>-1</sup>; M06-2X-D3/def2-TZVPP/IEFPCM//TPSS-D2/6-31G(d)/IEFPCM] for the Formation of Different Reactant Complexes **5–7** in the Henry Reaction between Benzaldehyde (**1**) and Nitronate Anion **2**



slightly endergonic ( $\Delta G = 0.9$  kcal mol<sup>-1</sup>). A similar finding of exothermic but endergonic binding has also been observed for the coordination of esters to diaryl thioureas.<sup>21</sup> An alternative conformation of the thiourea–benzaldehyde complex in which three hydrogen bonds are formed between the two molecules was found to be 4.6 kcal mol<sup>-1</sup> higher in energy, and the complex with the maximum of four hydrogen bonds was located 7.9 kcal mol<sup>-1</sup> higher in energy (see the Supporting Information for more details).

In the termolecular complex **7**, both benzaldehyde (**1**) and nitronate **2** are coordinated to the thiourea catalyst. The nitronate forms three hydrogen bonds to the catalyst (1.71, 1.74, and 1.81 Å; Figure 2) in the lowest-energy conformer, while the aldehyde participates in only one hydrogen bond (1.88 Å). The two carbon atoms involved in the Henry reaction are well-separated with a distance of 3.78 Å. Although the overall formation of the termolecular complex **7** is favored both enthalpically ( $-34.0$  kcal mol<sup>-1</sup>) and in terms of free energy ( $-9.2$  kcal mol<sup>-1</sup>), the binding of the second reactant (**1** or **2**) is less favorable by about 5 kcal mol<sup>-1</sup> because the termolecular complex is disfavored thermodynamically. Interestingly, the most stable complex **7** has the correct alignment for the formation of the minor *S* enantiomer of the final product, while complexes with the favorable *R* alignment are 5 kcal mol<sup>-1</sup> higher in energy. At almost the same energy as complex **7**, another conformer was located in which the nitronate is coordinated to all four thiourea NH groups and the aldehyde is loosely coordinated by dispersion interactions (see the Supporting Information for more details).

On the basis of our calculations, the formation of the bimolecular thiourea–nitronate complex **5** and a free benzaldehyde is preferred over the formation of the

termolecular complex **7** by 6 kcal mol<sup>-1</sup>. Therefore, the concentration of the latter in equilibrium will be very small, and aldehyde **1** will preferentially remain unbound. As a consequence, the termolecular complex **7** is not important for the energy profile, and the following discussion of the Henry reaction is based on the reaction of complex **5** with benzaldehyde (**1**).

**Transition States for the Thiourea-Catalyzed Henry Reaction.** Next, we calculated the transition states for the Henry reactions yielding the *R* and *S* products (Figure 3 and Scheme 5). The descriptor *R<sub>p</sub>* specifies the stereochemistry of the cyclophane-based bithiourea. This descriptor is omitted in the following discussion, and the prefixes (*R*) and (*S*) refer to the configuration of the Henry product. However, both transition states and the product complexes are diastereomers, since the *R<sub>p</sub>* catalyst is, of course, chiral.

In both transition states, the nitronate forms three hydrogen bonds to the bithiourea catalyst, while the aldehyde is held in place by one hydrogen bond (Figure 3). The hydrogen bonds

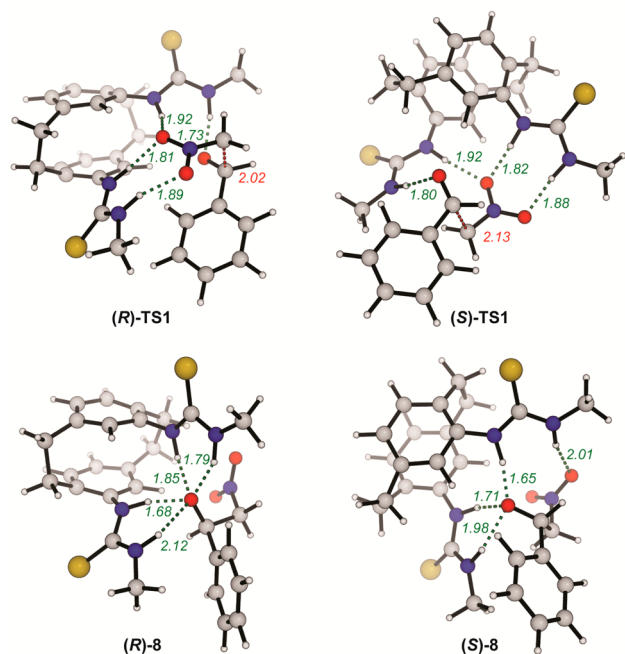


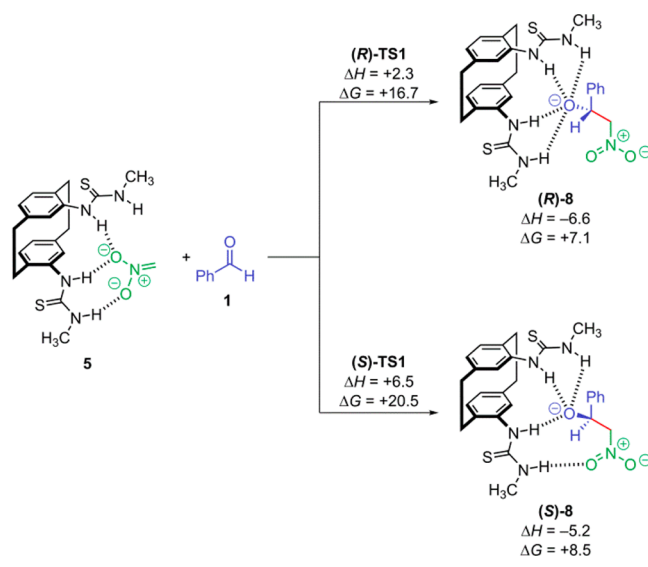
**Figure 3.** Calculated lowest-energy transition states **TS1** and products **8** [M06-2X-D3/def2-TZVPP/IEFPCM//TPSS-D2/6-31G(d)/IEFPCM] for the thiourea-catalyzed Henry reaction between nitronate anion **2** and benzaldehyde (**1**). All are complexed to the *R<sub>p</sub>* catalyst **3b**.

are almost identical for (*R*)-**TS1** and (*S*)-**TS1**, but the forming C–C bond is significantly shorter in the *R* transition state (2.02 Å) compared with the transition states for the *S* stereoisomer and the uncatalyzed reaction (2.13 and 2.11 Å, respectively). Within (*R*)-**TS1**, the nitronate and the aldehyde adopt a *gauche* conformation, which was calculated to be 1.2 kcal mol<sup>-1</sup> higher in energy for the uncatalyzed reaction (cf. *gauche-2* in Figure 1). The more favorable *anti* and *gauche-1* conformations (in the uncatalyzed reaction) are significantly higher in energy (>6 kcal mol<sup>-1</sup>; see the Supporting Information for more details) and less important for the reaction. A *gauche* conformation (*gauche-1* in Figure 1) is also preferred in (*S*)-**TS1**. Only for the *gauche-2* conformation for (*R*)-**TS1** [*gauche-1* for (*S*)-**TS1**] can an optimal hydrogen-bonding pattern be formed, while the negatively charged nitronate is almost uncoordinated for (*R*)-

**TS1** in the *anti* conformer. Therefore, the stabilization through hydrogen bonding to the catalyst compensates for the energetically less favorable *gauche* conformations in both transition states. A similar situation has been observed before for metal-catalyzed Henry reactions, in which the *gauche* conformation is stabilized in six-membered Zimmerman–Traxler-like transition states.<sup>15–17</sup>

The free energies of activation for the diastereomeric transition states were calculated to be 16.7 [(*R*)-**TS1**] and 20.5 kcal mol<sup>-1</sup> [(*S*)-**TS1**] with respect to the bimolecular thiourea–nitronate complex **5** and the uncoordinated aldehyde **1** (Scheme 5), revealing the large kinetic preference for the

**Scheme 5.** Reaction Enthalpies and Free Energies [in kcal mol<sup>-1</sup>; M06-2X-D3/def2-TZVPP/IEFPCM//TPSS-D2/6-31G(d)/IEFPCM] for the Thiourea-Catalyzed Henry Reaction between Benzaldehyde (**1**) and Nitronate Anion **2**



experimentally observed *R* product. This is also reflected in the different lengths of the hydrogen bonds in (*R*)- and (*S*)-**TS1**. While the hydrogen bonds to the nitro group are almost identical in the two structures, the hydrogen bond to the aldehyde is shorter in (*R*)-**TS1** (1.73 vs 1.80 Å; Figure 3). In comparison to the aldehyde–thiourea complex **6** (Figure 2), the hydrogen bonds are significantly shorter and indicate significant charge delocalization in the transition states.

**Validation of the Computational Method.** As the energy difference between (*R*)- and (*S*)-**TS1** determines the overall enantioselectivities, we employed these structures to verify our computational method. The most severe limitation could be the replacement of the 3,5-bis(trifluoromethyl)phenyl groups by methyl groups. It is well-known that this privileged aryl group influences the self-association and acidities of the catalysts because of the additional CH⋯S interaction, and to date no alkyl thiourea has ever successfully been employed as a catalyst.<sup>8a,21,23</sup> However, the computational description of the full system would not be feasible because of the size of the system and the large number of conformers. Therefore, we reoptimized the most stable conformers for (*R*)- and (*S*)-**TS1** with all of the 3,5-bis(trifluoromethyl)phenyl groups in place. As the relative differences in activation free energies calculated for the two systems were almost the same ( $\Delta\Delta G^\ddagger = 3.8$  kcal mol<sup>-1</sup> for **3b** and  $\Delta\Delta G^\ddagger = 4.3$  kcal mol<sup>-1</sup> for **3a**; see the

Supporting Information for more details), we can conclude that this simplification is justified for the elucidation of the origin of the enantioselectivity in these reactions despite the fact that the model catalyst would not be active under the experimental conditions.

Another limitation could be the small 6-31G(d) basis set used for the optimization and frequency calculations as well as the employed D2 correction<sup>24</sup> (implemented in Gaussian 09 revision C.01) instead of the newer D3 correction (implemented in the new Gaussian 09 revision D.01).<sup>25</sup> Both the use of the larger 6-31+G(d,p) basis set, which includes polarization functions on the hydrogen atoms as well as diffuse functions, and application of the D3 correction during the optimizations resulted in similar energy differences ( $\Delta\Delta G^\ddagger = 4.3$  and  $4.6$  kcal mol<sup>-1</sup>, respectively). As the energy difference between the diastereomeric transition states did not change significantly when the even larger quadruple- $\zeta$  def2-QZVP basis set<sup>26</sup> was used instead of the triple- $\zeta$  def2-TZVPP basis set ( $\Delta\Delta G^\ddagger = 3.6$  vs  $3.8$  kcal mol<sup>-1</sup>), we can conclude that our calculations do not suffer from large basis set superposition errors.<sup>27</sup>

**Product Complexes for the Thiourea-Catalyzed Henry Reaction.** In the most stable product complexes **8** (Figure 3 and Scheme 5), the negatively charged alcoholate is now stabilized through hydrogen bonding, similar to an oxyanion hole in enzymes.<sup>28</sup> In the most stable conformer of (*R*)-**8**, four hydrogen bonds are formed between the negatively charged oxygen atom and the two thiourea substructures, while the most stable conformer of diastereomeric (*S*)-**8** features the formation of three hydrogen bonds to the alcoholate and one hydrogen bond to the nitro group. A conformer of (*S*)-**8** with a similar hydrogen-bonding pattern as in (*R*)-**8** was also found for (*S*)-**8**; it is essentially isoenergetic to the conformer of (*S*)-**8** shown in Figure 3. The formation of each of the two diastereomeric product complexes (*R*)-**8** and (*S*)-**8** is exothermic ( $\Delta H = -6.6$  vs  $-5.2$  kcal mol<sup>-1</sup>) but (as a result of the unfavorable entropy) endergonic ( $\Delta G = +7.1$  vs  $+8.5$  kcal mol<sup>-1</sup>).

After the C–C bond is formed in the stereodetermining step, the alcoholate is protonated ( $\rightarrow$  **8–H**) and released from the catalyst. The ammonium salt of Hünig's base [ $pK_a(\text{Et}_3\text{NH}^+) = 9.0$  in DMSO]<sup>20d</sup> as well as the thiourea itself [ $pK_a = 11\text{--}13$  in DMSO]<sup>29</sup> could act as the proton source in this reaction. In the most stable neutral complexes **8–H** (Figure 4), hydrogen bonds between the nitro group as well as the hydroxy group and the thiourea stabilize the complex. The hydrogen bonds are

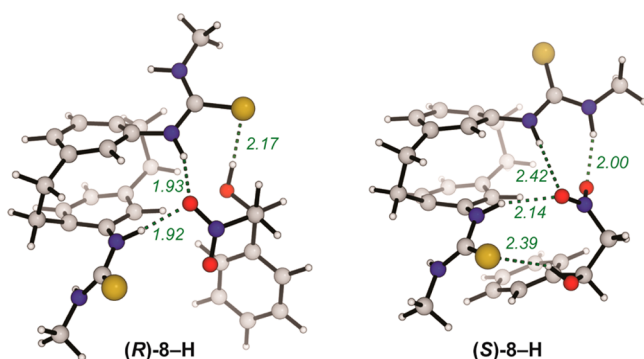
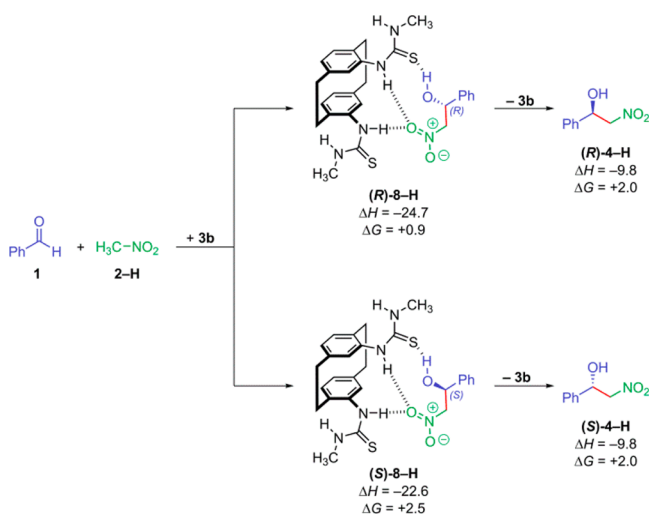


**Figure 4.** Calculated lowest-energy product complexes (*R*)-**8–H** and (*S*)-**8–H** [M06-2X-D3/def2-TZVPP/IEFPCM//TPSS-D2/6-31G(d)/IEFPCM] for the thiourea-catalyzed Henry reaction between nitronate anion **2** and benzaldehyde (**1**).

again significantly longer than in the anionic complexes **5**, **7**, and **8** and resemble more the neutral complex **5–H** (Figure 2).

The formation of the neutral product complexes **8–H** was calculated to be almost thermoneutral [ $\Delta G = 0.9$  kcal mol<sup>-1</sup> for (*R*)-**8–H** and  $2.5$  kcal mol<sup>-1</sup> for (*S*)-**8–H**; Figure 4 and Scheme 6]. For both enantiomers, the complexation to the

**Scheme 6. Overall Reaction Enthalpies and Free Energies [in kcal mol<sup>-1</sup>; M06-2X-D3/def2-TZVPP/IEFPCM//TPSS-D2/6-31G(d)/IEFPCM] for the Thiourea-Catalyzed Henry Reaction between Benzaldehyde (**1**) and Nitromethane (**2–H**)**



thiourea catalyst is very weak [or negligible for (*S*)-**8–H**], which indicates that the stabilization through hydrogen bonding is completely counterbalanced by the unfavorable entropy term  $-T\Delta S$ . The computed thermodynamics that indicate an almost thermoneutral reaction are again in agreement with the high reversibility of Henry reactions.<sup>17</sup>

**Comparison of the Uncatalyzed and Thiourea-Catalyzed Henry Reactions.** A comparison of the free energy profiles for the catalyzed and uncatalyzed Henry reactions is shown in Figure 5. Although the activation barriers are probably overestimated because of the neglect of ion pair formation with the ammonium ions, roughly the same stabilization should be obtained for the catalyzed and uncatalyzed reactions, and the energies reported in Figure 5 allow a qualitative discussion of both reactions. Our calculations reveal that the thiourea-catalyzed reaction is significantly faster than the uncatalyzed background reaction ( $\Delta\Delta G^\ddagger = 12.9$  kcal mol<sup>-1</sup>). This can be attributed to the large stabilization of the bimolecular complex **5**, which not only lowers the activation free energy for this transformation but also increases the acidity of the nitroalkane.

**Origin of the Enantioselectivity.** The relative energies of the transition states (*R*)- and (*S*)-TS1 parallel the stabilities of the corresponding product–thiourea complexes. As both transition states are significantly affected by charge delocalization, we employed the diastereomeric product complexes (*R*)-**8** and (*S*)-**8** to elucidate the origin of the selectivity. For both structures, we analyzed the contributions of distortion and hydrogen bonding, assuming that the difference in transition state energies will be of similar origin (Figure 6).

From the results in Table 1, one can conclude that the thiourea catalyst in (*R*)-**8** is slightly more distorted

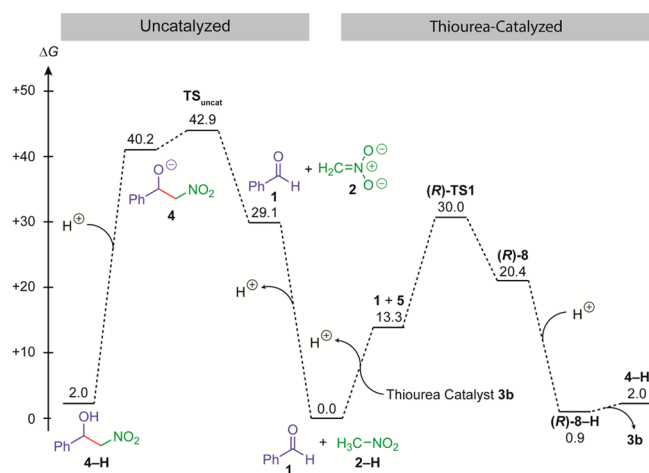


**Figure 5.** Comparison of the free energy profiles for the thiourea-catalyzed Henry reaction between benzaldehyde (**1**) and nitromethane (**2-H**) and the uncatalyzed background reaction [in kcal mol<sup>-1</sup>; see Figures 2–4 for structures; M06-2X-D3/def2-TZVPP/IEFPCM//TPSS-D2/6-31G(d)/IEFPCM].

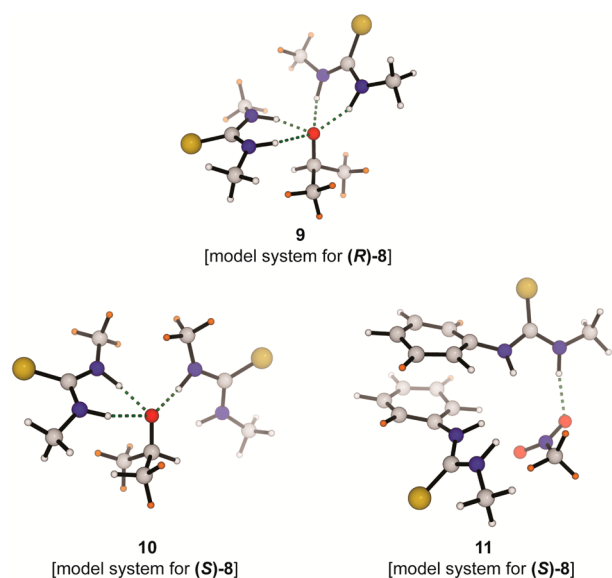


**Figure 6.** Model systems **9–11** employed for the assignment of hydrogen bonding in the product complexes **8**. Atoms marked in orange were allowed to relax during the optimization [M06-2X-D3/def2-TZVPP/IEFPCM//TPSS-D2/6-31G(d)/IEFPCM].

**Table 1.** Contributions of Distortion (dist) and Hydrogen Bonding (HB) to the Stabilities of the Product Complexes (**R**)-**8** and (**S**)-**8** [in kcal mol<sup>-1</sup>; M06-2X-D3/def2-TZVPP/IEFPCM//TPSS-D2/6-31G(d)/IEFPCM]

	( <b>R</b> )- <b>8</b>	( <b>S</b> )- <b>8</b>
$\Delta\Delta G$	0.0	+1.4
$\Delta\Delta E_{\text{dist}}(\text{thiourea})$	+2.7	0.0
$\Delta\Delta E_{\text{dist}}(\text{alcoholate})$	0.0	+2.0
$\Delta\Delta E_{\text{HB}}(\mathbf{9} \text{ vs } \mathbf{10})$	0.0	+4.1
$\Delta\Delta E_{\text{HB}}(\mathbf{11})$	– <sup>a</sup>	–1.1
$\Delta\Delta E_{\text{tot}}(\mathbf{9} \text{ vs } \mathbf{10})$	0.0	+2.3

<sup>a</sup>Substructure not present in (**R**)-**8**.

[ $\Delta\Delta E_{\text{dist}}(\text{thiourea})$ ] from its equilibrium geometry (**3b**) than in (**S**)-**8**. This is almost counterbalanced by the distortion of the

anionic Henry product [ $\Delta\Delta E_{\text{dist}}(\text{alcoholate})$ ] that is formed in that transformation, which is more distorted in (**S**)-**8**.

To assign the influence of the hydrogen bonds in the product complexes **8**, we employed the model systems **9–11** (Figure 6) derived from the optimized structures shown in Figure 3. These model systems reflect the hydrogen-bonding situation in the lowest-energy conformers (**R**)-**8** (model system **9**) and (**S**)-**8** (model systems **10** and **11**). These models contain all of the atoms that are also present in the full system, and those atoms were frozen for the optimization of the model systems. Only the terminal hydrogen atoms added for valence saturation were allowed to relax during the optimizations (orange spheres in Figure 6). This procedure allowed the estimation of the hydrogen-bond stabilization in both product complexes **8**.

Comparing the model systems **9** and **10**, a difference of 4.1 kcal mol<sup>-1</sup> was calculated for the different complexation energies of the negatively charged alcoholate and the thiourea [ $\Delta\Delta E_{\text{HB}}(\mathbf{9} \text{ vs } \mathbf{10})$  in Table 1]. Since these energies arise primarily from hydrogen bonding, this energy difference can be used as an estimate of the different contributions of hydrogen bonding in the product complexes **8**. As the thermodynamically less favored complex (**S**)-**8** contains an additional interaction between a nitro group and the thiourea subunit in the most stable conformer [which is not present in (**R**)-**8**], we additionally examined the model system **11** to account for that interaction [ $\Delta\Delta E_{\text{HB}}(\mathbf{11})$  in Table 1]. The calculated stabilizing contribution of 1.1 kcal mol<sup>-1</sup> is entirely attributed to dispersion effects, as the electronic energy without Grimme's D3 correction is essentially zero (see the Supporting Information for more details). Combining the contributions arising from distortion ( $\Delta\Delta E_{\text{dist}}$ ) and hydrogen bonding ( $\Delta\Delta E_{\text{HB}}$ ), a difference of 2.3 kcal mol<sup>-1</sup> ( $\Delta\Delta E_{\text{tot}}$ ) is expected for the diastereomeric product complexes. Compared to the calculated relative free energies (1.4 kcal mol<sup>-1</sup>), this value is in reasonable agreement considering the choice of the model system, and similar differences are expected for the transition states: stronger hydrogen bonding within (**R**)-**TS1** as well as a later transition state and thereby a better stabilization of the negative charge through hydrogen bonding to the aldehyde (1.73 vs 1.80 Å; see Figure 3 above) render (**R**)-**TS1** more stable than the diastereomeric (**S**)-**TS1**. Similar conclusions have previously been drawn for other thiourea-catalyzed reactions such as ketone cyanosilylations and imine hydrocyanations.<sup>34</sup>

On the basis of our computational results presented in Schemes 4–6, the formation of the (**R**)-alcohol is preferred kinetically. We calculated a kinetic preference of 3.8 kcal mol<sup>-1</sup>, which is slightly larger than the difference in reaction free energies ( $\Delta\Delta G = 1.4\text{--}1.6$  kcal mol<sup>-1</sup>). The stereoselectivity predicted here, > 99% ee, is considerably higher than the experimentally observed 90% ee. The Henry reaction is reversible, and consequently, the stereoselectivity may gradually erode with time. This may explain why our computed stereoselectivity is higher than that found experimentally.

## CONCLUSIONS

We have analyzed the Henry reaction between benzaldehyde (**1**) and nitromethane anion (**2**) catalyzed by novel cyclophane-based bithiourea **3b** using density functional theory. On the basis of our calculations, the Henry reaction occurs between a thiourea–nitronate complex and the uncoordinated aldehyde. The formation of the experimentally observed major stereoisomer is preferred kinetically as a result of a better hydrogen

arrangement. As the Henry reaction is reversible, the calculated high stereoselectivity may erode with time.

## ■ COMPUTATIONAL DETAILS

Although it is known that the 3,5-bis(trifluoromethyl)phenyl groups have an influence on the self-association and the acidities of the thiourea catalyst,<sup>8a,21,23</sup> the computational investigation was carried out with the simplified catalyst **3b** in which the aryl substituent was replaced by a methyl group in order to reduce the system to a reasonable size. This modification is not expected to have a large influence on the calculated transition states and product complexes that are important for the elucidation of the origin of the enantioselectivity in these reactions (see above in Results and Discussion).

The conformational space of all intermediates for the thiourea-catalyzed Henry reaction was explored using the OPLS-2005 force field<sup>50</sup> and a modified Monte Carlo search routine implemented in MacroModel version 9.9.<sup>31</sup> An energy cutoff of 20 kcal mol<sup>-1</sup> was used for the conformational analysis, and structures with heavy-atom RMSDs less than 1–2 Å after the initial force field optimization were assumed to be the same conformer. Because of the large number of conformers that were sampled by this procedure, a comprehensive set of conformers (up to 80 for some intermediates) was generated. The remaining structures were subsequently optimized employing the meta-GGA functional TPSS<sup>32</sup> with Grimme's D2 dispersion correction,<sup>24</sup> the double- $\zeta$  6-31G(d) basis set, and density fitting. Solvation by tetrahydrofuran was taken into account by using the integral equation formalism polarizable continuum model (IEFPCM) for all calculations (optimizations, frequencies, and single-point energies).<sup>33</sup> It has recently been shown that the use of a polarizable continuum model does not have a large impact on the calculated frequencies but is necessary for the location of transition states in some cases.<sup>34</sup> Vibrational analysis verified that each structure was a minimum or a transition state. Thermal corrections were calculated from unscaled harmonic vibrational frequencies at the same level of theory for a standard state of 1 mol L<sup>-1</sup> and 298.15 K. Entropic contributions to the reported free energies were calculated from partition functions evaluated with Truhlar's quasiharmonic approximation.<sup>34</sup> This method uses the same approximations as the usual harmonic oscillator approximation except that all vibrational frequencies lower than 100 cm<sup>-1</sup> are set equal to 100 cm<sup>-1</sup> to correct for the breakdown of the harmonic oscillator approximation for low frequencies. Electronic energies were subsequently obtained from single-point calculations on the TPSS-D2 geometries employing the meta-hybrid M06-2X functional,<sup>35</sup> the large triple- $\zeta$  def2-TZVPP basis set,<sup>26</sup> IEFPCM for tetrahydrofuran, and Grimme's D3 dispersion correction (zero-damping),<sup>25</sup> a level expected to give accurate energies.<sup>36</sup> The calculated enthalpies and free energies refer to the lowest-energy conformer and are almost identical to those obtained from Boltzmann-averaged ensembles. An ultrafine grid corresponding to 99 radial shells and 590 angular points was used throughout this study for numerical integration of the density.<sup>37</sup> All of the DFT calculations were performed with Gaussian 09,<sup>38</sup> and the additional D3 corrections for the single-point calculations were carried out with Grimme's DFT-D3 program.<sup>25</sup>

## ■ ASSOCIATED CONTENT

### Supporting Information

Cartesian coordinates, energies of all reported structures, and details of computational methods. This material is available free of charge via the Internet at <http://pubs.acs.org>.

## ■ AUTHOR INFORMATION

### Corresponding Authors

\*E-mail: [mbreugst@uni-koeln.de](mailto:mbreugst@uni-koeln.de)

\*E-mail: [houk@chem.ucla.edu](mailto:houk@chem.ucla.edu)

## Notes

The authors declare no competing financial interest.

## ■ ACKNOWLEDGMENTS

We are grateful to the Alexander von Humboldt Foundation (Feodor Lynen Scholarship to M.B.), the Fonds der Chemischen Industrie (Liebig Scholarship to M.B.), and the National Science Foundation (CHE-0548209 to K.N.H.) for financial support of this research. This work used the Extreme Science and Engineering Discovery Environment (XSEDE), which is supported by National Science Foundation Grant OCI-1053575, resources from the UCLA Institute for Digital Research and Education (IDRE), and the Cologne High Efficiency Operating Platform for Sciences (CHEOPS). We thank Dr. Arne Dieckmann and Dr. Yu-hong Lam for helpful discussions

## ■ REFERENCES

- (1) Kelly, T. R.; Meghani, P.; Ekkundi, V. S. *Tetrahedron Lett.* **1990**, *31*, 3381–3384.
- (2) (a) Etter, M. C. *Acc. Chem. Res.* **1990**, *23*, 120–126. (b) Etter, M. C.; Urbanczyk-Lipkowska, Z.; Zia-Ebrahimi, M.; Panunto, T. W. *J. Am. Chem. Soc.* **1990**, *112*, 8415–8426.
- (3) Curran, D. P.; Kuo, L. H. *J. Org. Chem.* **1994**, *59*, 3259–3261.
- (4) (a) Sigman, M. S.; Jacobsen, E. N. *J. Am. Chem. Soc.* **1998**, *120*, 4901–4902. (b) Vachal, P.; Jacobsen, E. N. *J. Am. Chem. Soc.* **2002**, *124*, 10012–10014.
- (5) (a) Schreiner, P. R.; Wittkopp, A. *Org. Lett.* **2002**, *4*, 217–220. (b) Wittkopp, A.; Schreiner, P. R. *Chem.—Eur. J.* **2003**, *9*, 407–414. (c) Schreiner, P. R. *Chem. Soc. Rev.* **2003**, *32*, 289–296.
- (6) (a) Berkessel, A.; Gröger, H. *Asymmetric Organocatalysis—From Biomimetic Concepts to Applications in Asymmetric Synthesis*; Wiley-VCH: Weinheim, Germany, 2005. (b) *Hydrogen Bonding in Organic Synthesis*; Pihko, P. M., Ed.; Wiley-VCH: Weinheim, Germany, 2009. (c) Takemoto, Y. *Org. Biomol. Chem.* **2005**, *3*, 4299–4306. (d) Taylor, M. S.; Jacobsen, E. N. *Angew. Chem., Int. Ed.* **2006**, *45*, 1520–1543. (e) Doyle, A. G.; Jacobsen, E. N. *Chem. Rev.* **2007**, *107*, 5713–5743. (f) Yu, X.; Wang, W. *Chem.—Asian J.* **2008**, *3*, 516–532. (g) Zhang, Z.; Schreiner, P. R. *Chem. Soc. Rev.* **2009**, *38*, 1187–1198. (h) Takemoto, Y. *Chem. Pharm. Bull.* **2010**, *58*, 593–601. (i) Takemoto, Y.; Inokuma, T. In *Asymmetric Synthesis II*; Christmann, M., Bräse, S., Eds.; Wiley-VCH: Weinheim, Germany, 2012; pp 233–237. (7) *Enzyme Catalysis in Organic Synthesis*, 2nd ed.; Drauz, K., Waldmann, H., Eds.; Wiley-VCH: Weinheim, Germany, 2002.
- (8) (a) Kotke, M.; Schreiner, P. R. In *Hydrogen Bonding in Organic Synthesis*; Pihko, P. M., Ed.; Wiley-VCH: Weinheim, Germany, 2009; pp 141–351. (b) Okino, T.; Hoashi, Y.; Takemoto, Y. *J. Am. Chem. Soc.* **2003**, *125*, 12672–12673. (c) Sohtome, Y.; Hashimoto, Y.; Nagasawa, K. *Adv. Synth. Catal.* **2005**, *347*, 1643–1648. (d) Shi, Y.-L.; Shi, M. *Adv. Synth. Catal.* **2007**, *349*, 2129–2135.
- (9) (a) Sohtome, Y.; Tanatani, A.; Hashimoto, Y.; Nagasawa, K. *Tetrahedron Lett.* **2004**, *45*, 5589–5592. (b) Zhang, Y.; Liu, Y.-K.; Kang, T.-R.; Hu, Z.-K.; Chen, Y.-C. *J. Am. Chem. Soc.* **2008**, *130*, 2456–2457. (c) De, C. K.; Klauber, E. G.; Seidel, D. *J. Am. Chem. Soc.* **2009**, *131*, 17060–17061. (d) Tan, B.; Hernández-Torres, G.; Barbas, C. F., III. *J. Am. Chem. Soc.* **2011**, *133*, 12354–12357.
- (10) Berkessel, A.; Roland, K.; Neudörfl, J. M. *Org. Lett.* **2006**, *8*, 4195–4198.
- (11) (a) Fleming, E. M.; McCabe, T.; Connon, S. J. *Tetrahedron Lett.* **2006**, *47*, 7037–7042. (b) Liu, X.-G.; Jiang, J.-J.; Shi, M. *Tetrahedron: Asymmetry* **2007**, *18*, 2773–2781. (c) Rampalakos, C.; Wulff, W. D. *Adv. Synth. Catal.* **2008**, *350*, 1785–1790. (d) Allu, S.; Selvakumar, S.; Singh, V. K. *Tetrahedron Lett.* **2010**, *51*, 446–448.
- (12) Kitagaki, S.; Ueda, T.; Mukai, C. *Chem. Commun.* **2013**, *49*, 4030–4032.
- (13) (a) Schneider, J. F.; Falk, F. C.; Fröhlich, R.; Paradies, J. *Eur. J. Org. Chem.* **2010**, 2265–2269. (b) Schneider, J. F.; Fröhlich, R.;

Paradies, J. *Synthesis* **2010**, 3486–3492. (c) Schneider, J. F.; Fröhlich, R.; Paradies, J. *Isr. J. Chem.* **2012**, *52*, 76–91.

(14) Sohtome, Y.; Nagasawa, K. *Synlett* **2010**, 1–22.

(15) (a) Seebach, D.; Beck, A. K.; Lehr, F.; Weller, T.; Colvin, E. *Angew. Chem., Int. Ed. Engl.* **1981**, *20*, 397–399. (b) Seebach, D.; Beck, A. K.; Mukhopadhyay, T.; Thomas, E. *Helv. Chim. Acta* **1982**, *65*, 1101–1133.

(16) Lecea, B.; Arrieta, A.; Morao, I.; Cossío, F. P. *Chem.—Eur. J.* **1997**, *3*, 20–28.

(17) Ono, N. *The Nitro Group in Organic Synthesis*; Wiley-VCH: New York, 2001.

(18) Hammar, P.; Marcelli, T.; Hiemstra, H.; Himo, F. *Adv. Synth. Catal.* **2007**, *349*, 2537–2548.

(19) Wheeler, S. E.; Moran, A.; Pieniazek, S. N.; Houk, K. N. *J. Phys. Chem. A* **2009**, *113*, 10376–10384.

(20) (a) Pearson, R. G.; Dillon, R. L. *J. Am. Chem. Soc.* **1953**, *75*, 2439–2443. (b) Hall, H. K. *J. Am. Chem. Soc.* **1957**, *79*, 5441–5444. (c) Matthews, W. S.; Bares, J. E.; Bartmess, J. E.; Bordwell, F. G.; Cornforth, F. J.; Drucker, G. E.; Margolin, Z.; McCallum, R. J.; McCollum, G. J.; Vanier, N. R. *J. Am. Chem. Soc.* **1975**, *97*, 7006–7014. (d) Kolthoff, I. M.; Chantooni, M. K.; Bhowmik, S. *J. Am. Chem. Soc.* **1968**, *90*, 23–28.

(21) Lippert, K. M.; Hof, K.; Gerbig, D.; Ley, D.; Hausmann, H.; Guenther, S.; Schreiner, P. R. *Eur. J. Org. Chem.* **2012**, 5919–5927.

(22) (a) Zuend, S. J.; Jacobsen, E. N. *J. Am. Chem. Soc.* **2007**, *129*, 15872–15883. (b) Zuend, S. J.; Jacobsen, E. N. *J. Am. Chem. Soc.* **2009**, *131*, 15358–15374.

(23) (a) Okino, T.; Hoashi, Y.; Takemoto, Y. *Tetrahedron Lett.* **2003**, *44*, 2817–2821. (b) Zhang, Z.; Lippert, K. M.; Hausmann, H.; Kotke, M.; Schreiner, P. R. *J. Org. Chem.* **2011**, *76*, 9764–9776.

(24) Grimme, S. *J. Comput. Chem.* **2006**, *27*, 1787–1799.

(25) Grimme, S.; Antony, J.; Ehrlich, S.; Krieg, H. *J. Chem. Phys.* **2010**, *132*, No. 154104.

(26) Weigend, F.; Ahlrichs, R. *Phys. Chem. Chem. Phys.* **2005**, *7*, 3297–3305.

(27) Risthaus, T.; Grimme, S. *J. Chem. Theory Comput.* **2013**, *9*, 1580–1591.

(28) (a) Nelson, D. L.; Cox, M. M. *Lehninger Principles of Biochemistry*, 4th ed.; Freeman: New York, 2005. (b) Kotke, M.; Schreiner, P. R. *Synthesis* **2007**, 779–790.

(29) Jakab, G.; Tancon, C.; Zhang, Z.; Lippert, K. M.; Schreiner, P. R. *Org. Lett.* **2012**, *14*, 1724–1727.

(30) Banks, J. L.; Beard, H. S.; Cao, Y.; Cho, A. E.; Damm, W.; Farid, R.; Felts, A. K.; Halgren, T. A.; Mainz, D. T.; Maple, J. R.; Murphy, R.; Philipp, D. M.; Repasky, M. P.; Zhang, L. Y.; Berne, B. J.; Friesner, R. A.; Gallicchio, E.; Levy, R. M. *J. Comput. Chem.* **2005**, *26*, 1752–1780.

(31) *MacroModel*, version 9.9; Schrödinger, LLC: New York, 2012.

(32) Tao, J.; Perdew, J. P.; Staroverov, V. N.; Scuseria, G. E. *Phys. Rev. Lett.* **2003**, *91*, No. 146401.

(33) Cancès, E.; Mennucci, B.; Tomasi, J. *J. Chem. Phys.* **1997**, *107*, 3032–3041.

(34) Ribeiro, R. F.; Marenich, A. V.; Cramer, C. J.; Truhlar, D. G. *J. Phys. Chem. B* **2011**, *115*, 14556–14562.

(35) Zhao, Y.; Truhlar, D. G. *Theor. Chem. Acc.* **2008**, *120*, 215–241.

(36) Goerigk, L.; Grimme, S. *Phys. Chem. Chem. Phys.* **2011**, *13*, 6670–6688.

(37) Wheeler, S. E.; Houk, K. N. *J. Chem. Theory Comput.* **2010**, *6*, 395–404.

(38) Frisch, M. J.; Trucks, G. W.; Schlegel, H. B.; Scuseria, G. E.; Robb, M. A.; Cheeseman, J. R.; Scalmani, G.; Barone, V.; Mennucci, B.; Petersson, G. A.; Nakatsuji, H.; Caricato, M.; Li, X.; Hratchian, H. P.; Izmaylov, A. F.; Bloino, J.; Zheng, G.; Sonnenberg, J. L.; Hada, M.; Ehara, M.; Toyota, K.; Fukuda, R.; Hasegawa, J.; Ishida, M.; Nakajima, T.; Honda, Y.; Kitao, O.; Nakai, H.; Vreven, T.; Montgomery, J. A., Jr.; Peralta, J. E.; Ogliaro, F.; Bearpark, M.; Heyd, J. J.; Brothers, E.; Kudin, K. N.; Staroverov, V. N.; Kobayashi, R.; Normand, J.; Raghavachari, K.; Rendell, A.; Burant, J. C.; Iyengar, S. S.; Tomasi, J.; Cossi, M.; Rega, N.; Millam, J. M.; Klene, M.; Knox, J. E.; Cross, J. B.; Bakken, V.; Adamo, C.; Jaramillo, J.; Gomperts, R.; Stratmann, R. E.; Yazyev, O.;

Austin, A. J.; Cammi, R.; Pomelli, C.; Ochterski, J. W.; Martin, R. L.; Morokuma, K.; Zakrzewski, V. G.; Voth, G. A.; Salvador, P.; Dannenberg, J. J.; Dapprich, S.; Daniels, A. D.; Farkas, Ö.; Foresman, J. B.; Ortiz, J. V.; Cioslowski, J.; Fox, D. J. *Gaussian 09, Revision C.01*; Gaussian, Inc.: Wallingford, CT, 2009.